Supporting Information

Transformation of Alkatetrayne Monolayers into Nanoflatcables Studied by Ultraviolet Photoelectron Spectroscopy and Metastable Atom Electron Spectroscopy

Hayato Sanada,[†] Yuichiro Asoma,[†] Hiroyuki Ozaki,[*,†] Osamu Endo,[†] Hideaki Oike,[†]

Masashi Hasegawa,[‡] and Yasuhiro Mazaki[‡]

[†]Department of Organic and Polymer Materials Chemistry, Graduate School of Engineering, Tokyo University of Agriculture and Technology, Koganei, Tokyo 184-8588, Japan

[‡]Department of Chemistry, School of Sciences, Kitasato University, Sagamihara, Kanagawa 252-0373, Japan

UPS features due to the conjugated chains of NFC on graphite

In this study, the takeoff angle of electrons is fixed to 60°, and the substrate cannot be rotated around the surface normal. One might wonder if the top of the HOMO band and that of the HOMO−1 band located at the Γ point (see Figure 10C) are observed by UPS, because the electronic structure at the Γ point is reflected in normal emission UPS for a "2D system".[1] Despite its 2D periodicity in the geometric structure, NFC can be regarded as an alternate array of two different 1D conjugated systems, which is valid provided the electronic structures of the conjugated chains do not mix with those of the alkyl chains so much. This is the case for the HOMO (HOMO−1) band of PA$\pi^{\perp}$ (PD$\pi^{\perp}$) character as the wave function in Figure 9 tells us. In addition, we must take another fact into consideration: HOPG comprises graphite crystallites with their *ab* (or (0001)) planes parallel to the macroscopic surface, but the in-plane orientation of the crystallites is random.

To simplify the system, let us approximate the PA chains of NFC, along which the orbitals constituting the HOMO band are distributed, by straight lines and erase other chemical structures in mind; this leaves a set of parallel PA chains with a large spacing in every graphite crystallite. In such a "mostly erased" NFC domain on a certain graphite crystallite, the direction of the conjugated chains coincides with the *x* axis of the substrate ($\phi = 0°$) (see Figure S1). The angle η between the PA chain and the direction of photoelectrons emitted from there is 30°. In a domain of another crystallite where the PA chain is parallel to the *y* axis ($\phi = 90°$), $\eta = 90°$. When viewed from a PA chain, therefore, photoelectrons emitted into a cone with η ($30° \leq \eta \leq 90°$) will be detected in our experimental conditions.

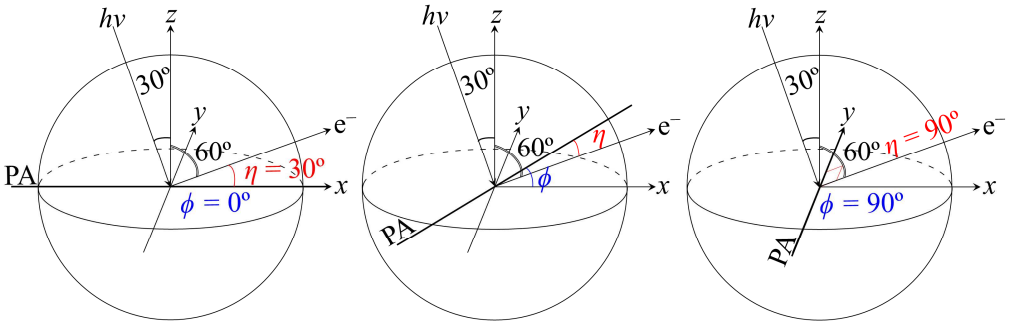

Figure S1 Photoemission from a PA chain laid flat with various in-plane orientaions. Coordinate axes are introduced so that electrons are emitted within the *xz* plane.

For a domain comprising PA chains with an azimuthal angle ϕ, η is given

$$\eta = \cos^{-1}\{(\sqrt{3}/2)\cos\phi\} \qquad (1)$$

The component of photoelectron momentum parallel to the PA direction, which is conserved and observed under these assumptions can be written as

$$k_{PA}\,\hbar = (2m\,E_k)^{1/2}\cos\eta \qquad (2)$$

If we approximate the dispersion curve of the HOMO band in Figure 10 by a cosine function and tentatively set E_k values for the top and the bottom at 17.1 and 13.3 eV, where mounts M_1 and M_4 appear in ΔUPS (Figure 8) (note that the bottom of the dispersion curve corresponds to mount M_4 in ΔDOS (Figure 10)), then we obtain

$$E_k/\mathrm{eV} = 1.9\cos(5.0\,k_{PA}/\mathrm{\AA}^{-1}) + 15.2 \qquad (3)$$

This curve is shown in Figure S2. When ϕ is decreased from 90° to 0° by 1°, each E_k vs k_{PA} plot for

$$E_k = (k_{PA}^2\hbar^2/2m\cos^2\eta) = (2\hbar^2/3m\cos^2\phi)\,k_{PA}^2 \qquad (4)$$

is superposed on the dispersion curve in Figure S2. A set of E_k and k_{PA} values for detectable electrons are determined from the points of intersection. Relation between E_k and ϕ is depicted in Figure S3. Expected UPS features for the HOMO band are synthesized in Figure S4(i) by superposing Gaussian functions with the same width and height at E_k values of all the intersection points in Figure S2 or at E_k values for ϕ ($0^\circ \le \phi \le 90^\circ$) with increments of 1° in Figure S3. Partial DOS for the HOMO alone is also shown in Figure S4(ii).

Compared with the partial DOS, the intensity of the synthesized UPS is nearly halved around the band bottom, which gives an extra peak at E_k higher than that for the bottom by 0.9 eV. This is accounted for by a fact that the intersection points of curves (3) and (4) do not reach the band bottom in the 3rd Brillouin zone (BZ): faster photoelectrons (17.1 eV < E_k ≤ 14.1 eV) are detected for three different ϕ values (1st to 3rd BZ) but slower ones (14.1 eV < E_k < 13.3 eV) for two ϕ values (1st and 2nd BZ). At any rate, Figure S4 indicates that the top of the HOMO band can be detected in our UPS. If we replace the PA chain in Figure S1 with a PD chain and adopt an approximate cosine curve for the HOMO−1 band, UPS features similar to Figure S4(i) are expected at a little lower E_k values. In reality, neither PA nor PD is a straight line but has a

zigzag shape and bridged with alkyl chains, and the acceptance angle of the analyzer is not infinitesimal as implicitly assumed. Such factors modify the energy distribution curves observed in the UPS, but they will essentially look like somewhat “blurred DOS” with partial depression.

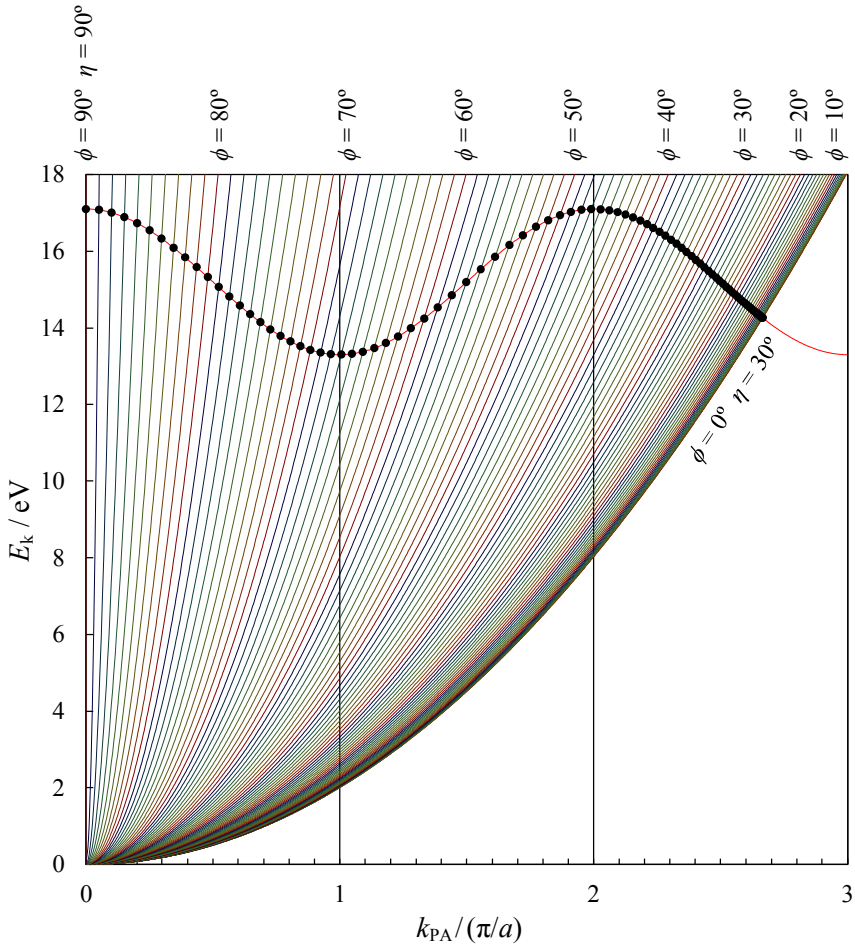

Figure S2 E_k vs k_{PA} plots for equations (3) and (4). The points of intersection correspond to detectable photoelectrons.

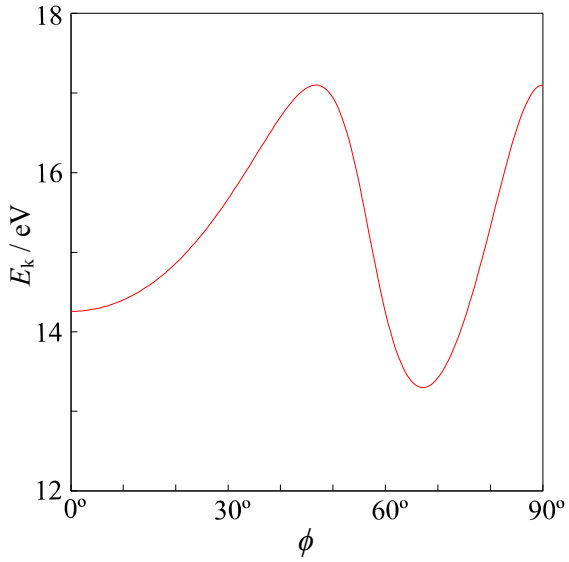

Figure S3 E_k vs ϕ plot for detectable photoelectrons originating in the HOMO band.

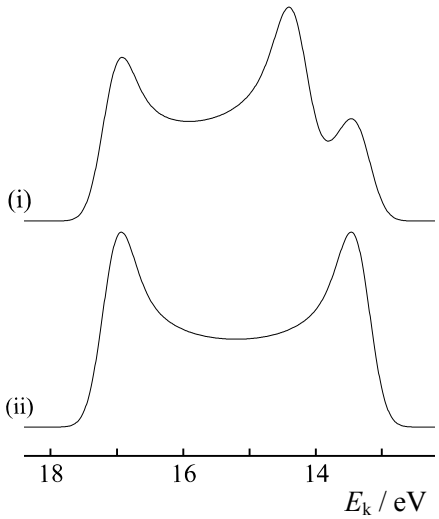

Figure S4 (i) Expected UPS features due to the HOMO band under the conditions of this study. (ii) Partial DOS for the HOMO band. Both curves are normalized with the integrated intensities.

Reference

(1) Lüth, H. *Solid Surfaces, Interfaces, and Thin Films*; Springer: Berlin, 2001; pp 265−328.